Automatic identification of Resting State Networks: An extended version of Multiple Template-Matching

Javier Guaje[a], Juan Molina[b], Jorge Rudas[a], Athena Demertzi[c], Lizette Heine[c], Luaba Tshibanda[c], Andrea Soddu[d], Steven Laureys[c] and Francisco Gómez[b]

[a] Computer Science Department, Universidad Nacional de Colombia, Bogotá, Colombia;
[b] Computer Science Department, Universidad Central de Colombia, Bogotá, Colombia;
[c] Cyclotron Research Center, University of Liege, Liege, Belgium;
[d] Physics and Astronomy Department, Western University, London, Canada

ABSTRACT

Functional magnetic resonance imaging in resting state (fMRI-RS) constitutes an informative protocol to investigate several pathological and pharmacological conditions. A common approach to study this data source is through the analysis of changes in the so called resting state networks (RSNs). These networks correspond to well-defined functional entities that have been associated to different low and high brain order functions. RSNs may be characterized by using Independent Component Analysis (ICA). ICA provides a decomposition of the fMRI-RS signal into sources of brain activity, but it lacks of information about the nature of the signal, i.e., if the source is artifactual or not. Recently, a multiple template-matching (MTM) approach was proposed to automatically recognize RSNs in a set of Independent Components (ICs). This method provides valuable information to assess subjects at individual level. Nevertheless, it lacks of a mechanism to quantify how much certainty there is about the existence/absence of each network. This information may be important for the assessment of patients with severely damaged brains, in which RSNs may be greatly affected as a result of the pathological condition. In this work we propose a set of changes to the original MTM that improves the RSNs recognition task and also extends the functionality of the method. The key points of this improvement is an standardization strategy and a modification of method's constraints that adds flexibility to the approach. Additionally, we also introduce an analysis to the trustworthiness measurement of each RSN obtained by using template-matching approach. This analysis consists of a thresholding strategy applied over the computed Goodness-of-Fit (GOF) between the set of templates and the ICs. The proposed method was validated on 2 two independent studies (Baltimore, 23 healthy subjects and Liege, 27 healthy subjects) with different configurations of MTM. Results suggest that the method will provide complementary information for characterization of RSNs at individual level.

Keywords: fMRI, resting-state, RSN, ICA, template-matching, artifact detection

1. INTRODUCTION

Functional magnetic resonance imaging at resting state (fMRI-RS) constitutes a robust protocol to investigate several pathological conditions, such as Alzheimer's disease, Schizophrenia, disorders of consciousness (DOC), as well as, different pharmacological states, for instance, sedation under different kinds of anesthetics.[1,2] Recent works suggest that brain at resting state is organized in well-defined spatio-temporal functional entities. At least ten of them have been consistently identified in healthy subjects: the default mode network (DMN), the executive control left and right networks (ECL and ECR), the salience (Sal.), the sensorimotor (Sen.), the auditory (Aud.), the three visual networks (Medial, Lateral and Occipital) and the cerebellum (Cer.)[3–6] A common approach to study altered brain conditions in fMRI-RS is through the analysis of changes in the connectivity of these resting-state networks (RSNs).[7]

A common approach to characterize these RSNs is by using Independent Component Analysis (ICA).[8] A method in which fMRI-RS signal is decomposed into statistically independent components, corresponding to spatial common structures and its associated behavior represented by a time-course. In most studies, RSNs are manually identified by looking for the independent component (IC) that better resembles specific well known spatial patterns associated to each RSN.[9] This process is time expensive and requires high levels of expertise, a factor that may greatly influence reproducibility.[10] Previous studies have approached the RSNs identification process by using template-matching (TM) techniques.[11] Multiple Template-Matching (MTM) is one of those studies and consists on compute a similarity measure between representations of each RSN and each one of the subject's ICs. Then, an optimization problem matches each RSN to the IC with highest visual similarity. This approach constitutes an automated and reproducible method for the RSNs identification task.[11–13]

RSNs identification has been also complemented with IC artifact detection methods. In these approaches, an spatio-temporal characterization method is computed for each IC, and a machine learning algorithm is used to discriminate components of artifactual and non-artifactual origin.[11,14,15] The combination of template-matching and artifact detection techniques has been used in the characterization of different pathological conditions (e.g. disorders of consciousness[11]) or pharmacological altered brain states (e.g. anesthesia induced by propofol[16]).

MTM and artifact detection have an important potential to be used in clinical environments, because their capacity to characterize individuals at the single level, in contrasts, to group based ICA analysis approaches.[17] Nevertheless, besides individual characterization, clinical applications require high level of reproducibly across different centers and a proper understanding of the method's parameters. In this work, we studied some of the minimum requirements that MTM methods[11] should accomplish in order to be used in future clinical settings. In particular, we study the consistency of the RSNs identification for fMRI-RS data acquired in different centers. For that, we propose an spatial and intensity normalization modification that enhances the method's reproducibility. Later, we explore the effect of different visual similarity measures between ICs and RSN templates, a critical parameter in the MTM algorithm, which may considerably affect its performance. Finally, we evaluate the sensibility of our method to changes in the similarity measure. Our results show that these extensions result in an approach that can have good potential to be used in the identification of RSNs at individual level in clinical environments.

2. MATERIALS AND METHODS

2.1 Participants and data acquisitions

Data from 27 healthy controls (14 women, mean age 47 ± 16 years) were used for this study. Previous written consent to participate in the study was obtained from all subjects. Each subject were instructed to close their eyes, relax without falling asleep and avoid any structured thinking (e.g., counting, singing, etc.). Then, fMRI-RS data were acquired in a 3T scanner in Erlangen, Germany. Three hundred fMRI volumes multislice $T2^*$-weighted functional images were captured (32 slices; repetition time = $2000ms$). The three initial volumes were discarded to avoid T1 saturation effects. Additionally a high resolution structural T1-weighted image was also acquired for anatomical reference.

Data from 1000 Functional Connectomes Project was also used. 1000 Functional Connectomes Project (http://fcon_1000.projects.nitrc.org) captures and manages collections of fMRI-RS data acquired in more than 30 independent studies from around the world. These heterogeneous samples of data offer the opportunity to study the reliability and reproducibility of resting-state oriented analysis.

In order to measure the overall performance of our approach we have tested our methods in Baltimore's dataset. This dataset is composed by 23 subjects (15 women, mean age 29 ± 5 years). fMRI-RS data were acquired under opened eyes condition in a 3T scanner in Baltimore, MD, USA. One hundred and twenty three fMRI volumes multislice $T2^*$-weighted functional images were captured (47 slices; repetition time = $2500ms$). The first five timepoints of each timeseries were discarded. For anatomical reference two high resolution structural images were also acquired.

2.2 Templates selection

RSNs templates were selected by an expert via visual inspection from a set of spatially independent components. These components were taken from 12 independently assessed controls (4 women, mean age 21 ± 3 years) scanned on a 3T scanner (32 slices; repetition time = $2460ms$). The templates were then checked by another expert for accuracy of structural labeling.

11th International Symposium on Medical Information Processing and Analysis, edited by Eduardo Romero, Natasha Lepore, Juan D. García-Arteaga, Jorge Brieva, Proc. of SPIE Vol. 9681, 96810V
 · doi: 10.1117/12.2211530

2.3 Preprocessing

Data was mostly preprocessed using Statistical Parametric Mapping version 8 (SPM8; http:www.fil.ion.ucl.ac.uk/spm). Preprocessing steps performed were: spatial realignment, coregistration of functional onto structural data, segmentation of structural data, normalization into MNI space and spatial smoothing with a Gaussian kernel of $8mm$. Large head motions,[18] noise spikes and spontaneous deep breaths were further corrected using ArtRepair (http://cibsr.stanford.edu/tools/ArtRepair/ArtRepair.htm).

2.4 Spatial Independent Component Analysis

Multiple Template-Matching (MTM) algorithm requires comparable entities to be performed. Given that each RSN template is a set of well defined brain regions, subject's fMRI volumes must be summarized in similar spatial maps. Although, there are many ways to accomplish that,[19,20] we have opted for a data oriented approach extensively used in the literature called Independent Component Analysis (ICA). This technique decompose fMRI signal into a set of Independent Components (ICs) of brain activity. Due to fMRI's spatial dimension is higher than the temporal one, we used spatial ICA (sICA), a variant which decompose the signal into maximally independent spatial maps.[21] For this task, we have selected the Infomax algorithm as implemented in GroupICA for fMRI toolbox (GIFT; http://icatb.sourceforge.net/). Between the parameters required by this algorithm we set the number of ICs as 30. Then, the component images (spatial maps) were calibrated to the raw data so the intensity values were in units of Percent Signal Change (PSC) from the mean.[22]

2.5 Extended Multiple Template Matching method

2.5.1 Components Normalization

Inter and intra-subject variability can be a hard condition to face, especially when protocols are changed. Clinical applications of resting-state (i.e. pathological and pharmacological studies), by its particular conditions, can be more prone to certain configurations. In order to offer a method that cover as much as possible this susceptibilities, our first contribution to the original MTM method is a normalization strategy.

Scanner related configurations, such as the number of slices are reflected in ICs. Therefore, the size of the spatial maps to be compared must be the same. PSC also induces inter and intra-variabilities that can alter Goodness-of-Fit (GOF) computation and consequently Template-Matching (TM) results. To diminish the effects of PCS related variability and in order to make the ICs comparable versus the RSNs templates, we have normalized the intensities of each image between 0 and 1 using the following equation:

$$C_N = \frac{C + abs(min(C))}{max(C) + abs(min(C))} \tag{1}$$

where C is the 3D volume corresponding to each one of the subject's ICs.

2.5.2 Identification of RSNs at individual level

Over the original MTM,[11] some changes has been proposed. First, the original method has been extended to allow compare not only ICs and templates, but compare two sets of spatial maps. Therefore, to overcome potentially concurrent assignations between images, the two original restrictions must be changed to:

(i) The set with fewer items must assign each one of its spatial maps to one of the other set.

(ii) Each one of the spatial maps of the set with more items can be assigned or not.

(iii) In case both sets have the same size, each one of the spatial maps must be assigned to a component of the other set.

Considering these constraints, we have that the TM optimization problem may be formulated as follows:

$$\begin{aligned} &\underset{x}{\text{maximize}} \sum_{i=1}^{M}\sum_{j=1}^{N} x_{i,j} g_{i,j} \\ &\text{subject to} \\ &\sum_{i=1}^{M} x_{i,j} \begin{cases} = 1, & N \leq M \\ \leq 1, & \text{otherwise} \end{cases} ; \forall j \in \mathbb{Z} \mid 1 \leq j \leq N \\ &\sum_{j=1}^{N} x_{i,j} \begin{cases} = 1, & M \leq N \\ \leq 1, & \text{otherwise} \end{cases} ; \forall i \in \mathbb{Z} \mid 1 \leq i \leq M \end{aligned} \tag{2}$$

where M and N are the respective sizes of each set, $g_{i,j}$ is a GOF measure that quantifies the level of visual similarity between two spatial maps and $x_{i,j} \in \{0,1\}$ is an assignation binary variable indicating the match between the map i and the map j. The proposed optimization problem was solved by using binary linear programming[23] as implemented in MATLAB Mixed-integer linear programming (MILP; intlinprog; http://www.mathworks.com/help/optim/ug/intlinprog.html). For our experimentation, we considered as similarity measure ($g_{i,j}$) the GOF proposed by Greicius et. al.,[24] which quantifies the average of the voxels falling in one of the maps and then subtracts the average of the voxels outside this map. The original method is complemented by relaxing the chosen GOF measure, this is, the extended method treats the similarity measure as a parameter. Reported results also include the Pearson correlation coefficient as a GOF measure.

By solving this problem we get a coupling between the binary RSNs templates and the ICs with highest global GOF (taking into account all templates simultaneously). Given that usually the number of ICs (30)[25] is larger or equal than the number of the templates, the first constraint ensured that all binary RSNs templates would be assigned. The second restriction forced a unique identification of each IC, overcoming potentially concurrent component assignations.

2.6 Components Classification

Each one of the assigned ICs were classified by its nature as artifactual or non-artifactual using a supervised machine learning algorithm. Specifically a binary classifier strategy using a Support Vector Machine (SVM) with a Radial Basis Function (RBF) kernel. The chosen implementation is the one made by the University of Waikato in Weka 3: Data Mining Software in Java[26] (http://www.cs.waikato.ac.nz/~ml/weka/), which works with LIBSVM - A Library for Support Vector Machines (https://www.csie.ntu.edu.tw/~cjlin/libsvm/). For the features vector we chose a novel approach called IC-fingerprint, which characterizes ICs as a multidimensional space of 11 descriptive measures,[14] 4 spatial based (degree of clustering, skewness, kurtosis, spatial entropy) and 7 temporal based (one-lag autocorrelation, temporal entropy, power of five frequency bands: 0-0.008 Hz, 0.008-0.02 Hz, 0.02-0.05 Hz, 0.05-0.1 Hz, and 0.1-0.25 Hz).

2.7 Thresholding procedure

Previously described optimization problem ensures a mutual assignation between an IC and a template, but does not provide any information about the level of certainty for the existence/absence of each RSN. This aspect is quite relevant on pathological subjects, where RSNs may be affected by the pathological condition, resulting on ICs with different spatial patterns to the ones originally assumed by the RSN templates.

In order to estimate the sensibility of the proposed method, we conducted a simple experiment. A thresholding strategy which assumes that the highest GOF per template is in fact a RSN. In contrast, the lowest GOF is taken as a mismatch in the assignation. Given these 2 assumptions, a threshold can be placed and its impact in RSNs detection can be measured.

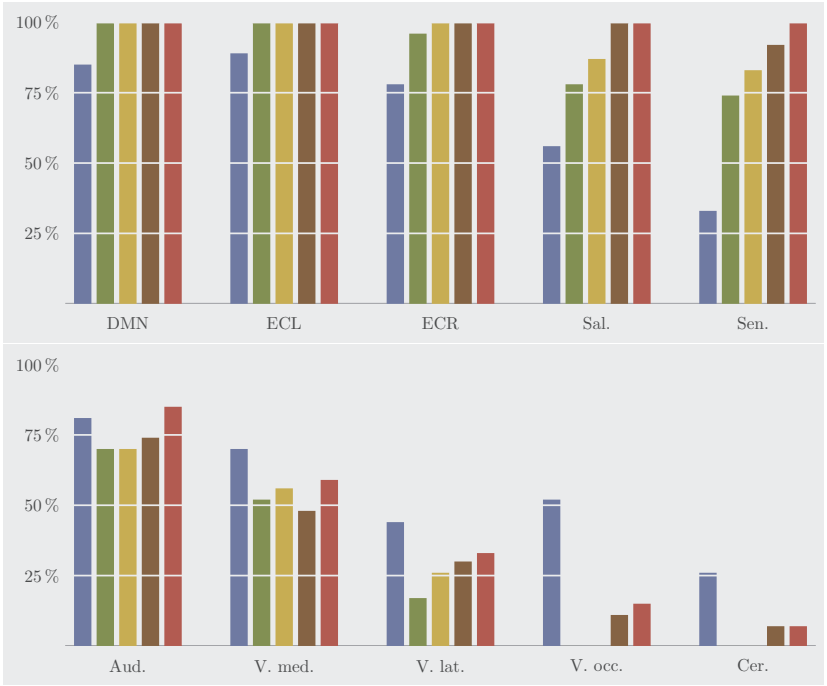

Figure 1. For each RSN, from left to right. First, results reported by Demertzi, Gómez, Laureys, Soddu, et. al. (Blue). Followed by the results for Baltimore's dataset, Pearson correlation coefficient in contrast with Greicius GOF[24] (Green and Yellow). Finally, fourth and fifth values were obtained for Liege's dataset, Pearson correlation coefficient versus Greicius GOF[24] (Brown and Red). In all cases, the applied procedure was: normalization, GOF computation, RSNs detection and Artifacts identification.

3. RESULTS

Figure 1 shows the results of the original MTM and the improvements achieved by extending the method and different sets of configurations. Mainly, by changing the visual similarity measure, but also by testing with different datasets. As observed in columns 1 and 5 of each RSN, the extended method shows a significant improvement in the detection for the first 5 networks (from 85%, 89%, 78%, 56% and 33% respectively to 100%). Auditory network also experiences a better detection (85% vs 81%). In the case of visual medial network, although shows a lower detection (59% vs 70%), it still has a good detection percentage. Visual lateral, visual occipital and cerebellum networks however, resulted in the lowest detected networks (33%, 15% and 7% respectively), even lower than original method (44%, 52% and 26% respectively). It is worth to say that one of the improvements is in the detection of the DMN (from 85% to 100%), a very used network to study pathologies such as Alzheimer's Disease (AD),[24] Disorders of Consciousness (DOC),[13,27] Schizophrenia,[28] among others.

Columns 2 and 3 of each RSN show the behavior of Pearson correlation coefficient in contrast with Greicius GOF[24] for Baltimore's data. Columns 4 and 5 exhibit a similar experiment for Liege's dataset. In both studies we found a good detection of RSNs, at least in the first 6 enumerated networks (greater than 70%). Regarding to similarity measures, Greicius GOF[24] exhibits a slightly better performance. Finally, columns 3 and 5 summarize the best performance achieved for each dataset. In both cases, Greicius GOF[24] reports better detections. Common behavior between both datasets includes a high detection of DMN, ECL and ECR (100%). Followed by Salience and Sensorimotor networks (between 80% and 100%), auditory network (between 70% and 85%) and lastly visual medial network (between 56% and 59%). Visual lateral, visual occipital and cerebellum networks were poorly detected (between 0% and 33%).

Figure 2 shows the effects of applying a set of thresholds over a normalized GOFs. From previously described results, we choose Greicius GOF[24] as the visual similarity measure.

4. CONCLUSIONS

In this work we have proposed a set of novelties to extend the MTM method. Results suggest that this approach can detect RSNs independent of the study's variability. In the case of Liege's study we have achieved an overall improvement over the original results,[11] same detection patterns were observed in Baltimore's dataset. From that, we can conclude that normalization process improves the reproducibility of the method and is ready to be applied in clinical environments (pathological and pharmacological populations) where visual identification is problematic. Additionally, we found that Greicius GOF[24] report better results than Pearson correlation coefficient. Future work includes the implementation of different similarity measures and as we suggested, evaluation of the method in patients.

ACKNOWLEDGMENT

This work was supported by the project "Caracterización de interacciones entre redes de descanso en pacientes con desórdenes de conciencia" from Universidad Central de Colombia, the Belgian National Funds for Scientic Research (FNRS), tinnitus Prize 2011 (FNRS 9.4501.12), the European Commission, the James McDonnell Foundation, the European Space Agency, Mind Science Foundation, the French Speaking Community Concerted Research Action, the Belgian interuniversity attraction pole, the Public Utility Foundation "Université Européenne du Travail", "Fondazione Europea di Ricerca Biomedica" and the University Hospital of Liége.

REFERENCES

[1] Bagshaw, A. P. and Cavanna, A. E., "Resting state networks in paroxysmal disorders of consciousness," *Epilepsy & Behavior* **26**(3), 290–294 (2013).

[2] Farb, N. A., Grady, C. L., Strother, S., Tang-Wai, D. F., Masellis, M., Black, S., Freedman, M., Pollock, B. G., Campbell, K. L., Hasher, L., et al., "Abnormal network connectivity in frontotemporal dementia: evidence for prefrontal isolation," *Cortex* **49**(7), 1856–1873 (2013).

[3] Damoiseaux, J., Rombouts, S., Barkhof, F., Scheltens, P., Stam, C., Smith, S. M., and Beckmann, C., "Consistent resting-state networks across healthy subjects," *Proceedings of the national academy of sciences* **103**(37), 13848–13853 (2006).

[4] Heine, L., Soddu, A., Gómez, F., Vanhaudenhuyse, A., Tshibanda, L., Thonnard, M., Charland-Verville, V., Kirsch, M., Laureys, S., and Demertzi, A., "Resting state networks and consciousness: alterations of multiple resting state network connectivity in physiological, pharmacological, and pathological consciousness states," *Frontiers in psychology* **3** (2012).

[5] Laird, A. R., Fox, P. M., Eickhoff, S. B., Turner, J. A., Ray, K. L., McKay, D. R., Glahn, D. C., Beckmann, C. F., Smith, S. M., and Fox, P. T., "Behavioral interpretations of intrinsic connectivity networks," *Journal of cognitive neuroscience* **23**(12), 4022–4037 (2011).

[6] Smith, S. M., Fox, P. T., Miller, K. L., Glahn, D. C., Fox, P. M., Mackay, C. E., Filippini, N., Watkins, K. E., Toro, R., Laird, A. R., et al., "Correspondence of the brain's functional architecture during activation and rest," *Proceedings of the National Academy of Sciences* **106**(31), 13040–13045 (2009).

[7] Fox, M. D. and Raichle, M. E., "Spontaneous fluctuations in brain activity observed with functional magnetic resonance imaging," *Nature Reviews Neuroscience* **8**(9), 700–711 (2007).

[8] Jafri, M. J., Pearlson, G. D., Stevens, M., and Calhoun, V. D., "A method for functional network connectivity among spatially independent resting-state components in schizophrenia," *Neuroimage* **39**(4), 1666–1681 (2008).

[9] Beckmann, C. F., DeLuca, M., Devlin, J. T., and Smith, S. M., "Investigations into resting-state connectivity using independent component analysis," *Philosophical Transactions of the Royal Society of London B: Biological Sciences* **360**(1457), 1001–1013 (2005).

[10] Storti, S. F., Formaggio, E., Nordio, R., Manganotti, P., Fiaschi, A., Bertoldo, A., and Toffolo, G. M., "Automatic selection of resting-state networks with functional magnetic resonance imaging," *Frontiers in neuroscience* **7** (2013).

[11] Demertzi, A., Gomez, F., Crone, J. S., Vanhaudenhuyse, A., Tshibanda, L., Noirhomme, Q., Thonnard, M., Charland-Verville, V., Kirsch, M., Laureys, S., et al., "Multiple fmri system-level baseline connectivity is disrupted in patients with consciousness alterations," *Cortex* **52**, 35–46 (2014).

[12] Norton, L., Hutchison, R., Young, G., Lee, D., Sharpe, M., and Mirsattari, S., "Disruptions of functional connectivity in the default mode network of comatose patients," *Neurology* **78**(3), 175–181 (2012).

[13] Vanhaudenhuyse, A., Noirhomme, Q., Tshibanda, L. J.-F., Bruno, M.-A., Boveroux, P., Schnakers, C., Soddu, A., Perlbarg, V., Ledoux, D., Brichant, J.-F., et al., "Default network connectivity reflects the level of consciousness in non-communicative brain-damaged patients," *Brain* **133**(1), 161–171 (2010).

[14] De Martino, F., Gentile, F., Esposito, F., Balsi, M., Di Salle, F., Goebel, R., and Formisano, E., "Classification of fmri independent components using ic-fingerprints and support vector machine classifiers," *Neuroimage* **34**(1), 177–194 (2007).

[15] Sui, J., Adali, T., Pearlson, G. D., and Calhoun, V. D., "An ica-based method for the identification of optimal fmri features and components using combined group-discriminative techniques," *Neuroimage* **46**(1), 73–86 (2009).

[16] Ramani, R., Qiu, M., Qadri, S., Gomez, F., Laureys, S., and Constable, R., "Propofol 2 microg/ml affects higher mental function networks in the brain," in [*Proceedings of the American Society of Anesthesiologists 2013*], (2013).

[17] Calhoun, V., Adali, T., Pearlson, G., and Pekar, J., "A method for making group inferences from functional mri data using independent component analysis," *Human brain mapping* **14**(3), 140–151 (2001).

[18] Power, J. D., Barnes, K. A., Snyder, A. Z., Schlaggar, B. L., and Petersen, S. E., "Spurious but systematic correlations in functional connectivity mri networks arise from subject motion," *Neuroimage* **59**(3), 2142–2154 (2012).

[19] Richiardi, J., Achard, S., Bunke, H., and Van De Ville, D., "Machine learning with brain graphs: predictive modeling approaches for functional imaging in systems neuroscience," *Signal Processing Magazine, IEEE* **30**(3), 58–70 (2013).

[20] Varoquaux, G. and Craddock, R. C., "Learning and comparing functional connectomes across subjects," *NeuroImage* **80**, 405–415 (2013).

[21] McKeown, M. J., Makeig, S., Brown, G. G., Jung, T.-P., Kindermann, S. S., Bell, A. J., and Sejnowski, T. J., "Analysis of fmri data by blind separation into independent spatial components," tech. rep., DTIC Document (1997).

[22] Calhoun, V., Adali, T., Stevens, M., Kiehl, K., and Pekar, J., "Semi-blind ica of fmri: a method for utilizing hypothesis-derived time courses in a spatial ica analysis," *Neuroimage* **25**(2), 527–538 (2005).

[23] Grötschel, M. and Holland, O., "Solving matching problems with linear programming," *Mathematical Programming* **33**(3), 243–259 (1985).

[24] Greicius, M. D., Srivastava, G., Reiss, A. L., and Menon, V., "Default-mode network activity distinguishes alzheimer's disease from healthy aging: evidence from functional mri," *Proceedings of the National Academy of Sciences of the United States of America* **101**(13), 4637–4642 (2004).

[25] Abou-Elseoud, A., Starck, T., Remes, J., Nikkinen, J., Tervonen, O., and Kiviniemi, V., "The effect of model order selection in group pica," *Human brain mapping* **31**(8), 1207–1216 (2010).

[26] Hall, M., Frank, E., Holmes, G., Pfahringer, B., Reutemann, P., and Witten, I. H., "The weka data mining software: an update," *ACM SIGKDD explorations newsletter* **11**(1), 10–18 (2009).

[27] Fernández-Espejo, D., Soddu, A., Cruse, D., Palacios, E. M., Junque, C., Vanhaudenhuyse, A., Rivas, E., Newcombe, V., Menon, D. K., Pickard, J. D., et al., "A role for the default mode network in the bases of disorders of consciousness," *Annals of neurology* **72**(3), 335–343 (2012).

[28] Öngür, D., Lundy, M., Greenhouse, I., Shinn, A. K., Menon, V., Cohen, B. M., and Renshaw, P. F., "Default mode network abnormalities in bipolar disorder and schizophrenia," *Psychiatry Research: Neuroimaging* **183**(1), 59–68 (2010).

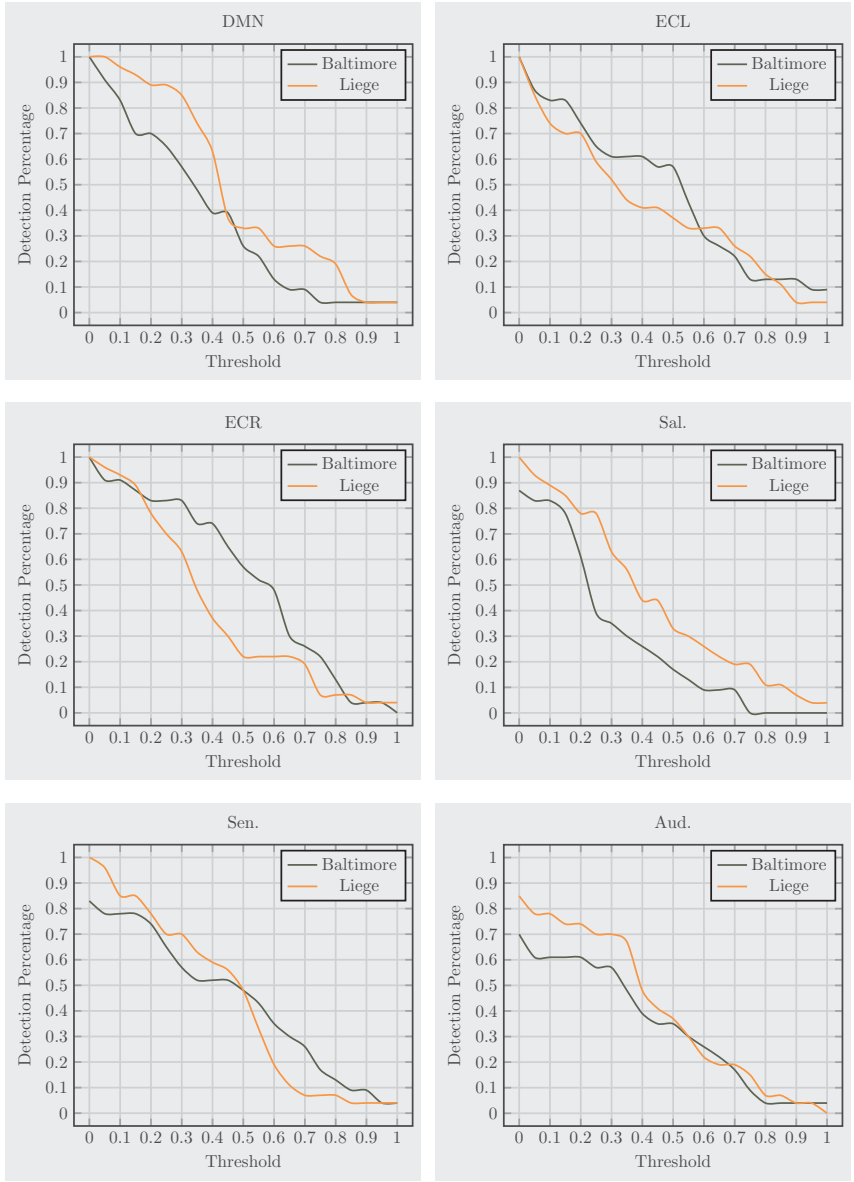

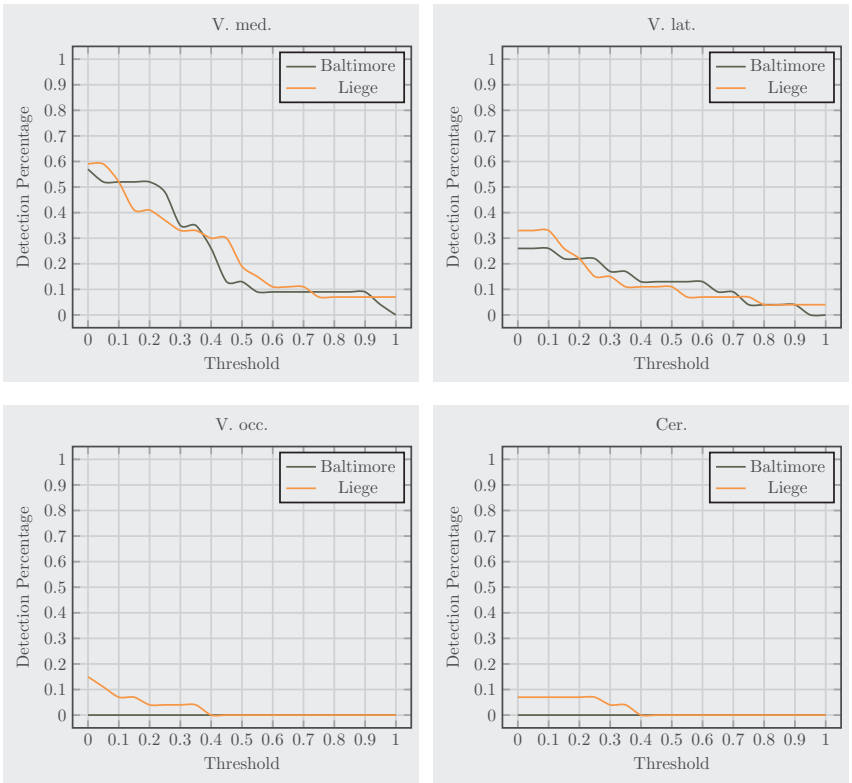

Figure 2. Effects of thresholding procedure (Subsection 2.7) in each RSN. Abscissa axis represents a set of normalized thresholds and ordinate axis shows the impact of these thresholds in the detection percentage. These results were obtained using Greicius GOF[24] as the visual similarity measure.